WIND TUNNEL WALL INTERFERENCE IN A TEST SECTION WITH VENTILATED WALLS

ICAS-80-23.5

Hideo Sawada
Aerospace Engineer
National Aerospace Laboratory
Tokyo, Japan

Abstract

Quite a new approach to the ventilated wind tunnel wall interference problem is proposed in this paper, in which, instead of assuming a doubtful mathematical model for the ventilated wall characteristics, velocity components of flow near the walls inside a test section are used as boundary conditions for solving a boundary value problem of the flow field. Then the wall interference on a wing model installed in a test section is estimated no matter how complex the wall characteristics may be. Besides, the velocity need not be measured in detail on the whole tunnel walls. Various quantities related to wall interference can be estimated with sufficient accuracy if only transversal lower harmonics of the streamwise distributions are available. The effect of suction from the side walls in a two-dimensional test is also investigated. The above method for calculating blockage and lift interference corrections was applied to a two-dimensional test section configuration of the NAL 2m × 2m transonic wind tunnel. The configuration was such that the open area ratio of side walls was set at 0 % and that of the top and bottom walls at 20 %. The lift interference parameters and the blockage factor ratio, which are traditionally used in wall interference correction methods, were evaluated in a reasonable manner by using the formulation derived in the present theory. The values of these parameters thus obtained were shown to depend on the lift coefficient but not so sensitively on uniform Mach number between 0.6 and 0.8, nor on the difference in the tested airfoil sections. Consequently, it becomes possible by the use of the above characteristics to make corrections without measuring the pressure distributions near the walls each time.

I. Introduction

The wall interference problem still remains to be solved in a proper manner theoretically as well as empirically as far as transonic wind tunnel equipped with ventilated walls is concerned. It becomes, however, more and more urgent today to solve this problem because more accurate test data are needed to design aerodynamically more efficient aircraft. This problem is difficult to solve mainly because the characteristics of ventilated walls are extremely complex; they depend on the flow conditions at the walls which are far from being expressed by a simple mathematical model. In this connection, the theoretical models proposed in any previous methods are all inadequate to simulate the real flow in a test section.[1] This may be properly inferred from the recent experiments of M. Mokry[2] and J. Kacprzynski[3] in Canada. Considering the above fact, quite different approaches to this problem have been prposed recently by several[4]-[12] authors. They all need static pressure or velocity components of the flow near the walls inside a test section. A common feature of these methods is to use those quantities as boundary conditions for solving a boundary value problem, instead of assuming a doubtful mathematical model for the ventilated wall characteristics. The present author has also proposed an approach.[7] Of these papers, only two deal with three-dimensional wall interference. Only the case of a test section with solid side walls was studied in Ref.(5), while the case with four ventilated walls was studied by the present author in Ref.(8). In this paper, the approach in Ref.(8) is developed further and the effect of suction from side walls of a two-dimensional wind tunnel is investigated in detail. Besides, the lift interference parameters[13] and the blockage factor ratio[14]-[15] are given, which were evaluated from test

data by the aid of the formulation derived in the present theory in the case of the NAL 2m × 2m transonic wind tunnel with two-dimensional configured test section.

Notations

A : area of wing planform transformed by Eq.(4)
B_n : Bernoulli number
b : semi-span length of wing transformed by Eq.(4)
C : cross-sectional area of tunnel
C_L : lift coefficient
C_D : drag coefficient
C_p : pressure coefficient in a tunnel
$\tilde{C}_p$: pressure coefficient in free air
c : airfoil chord length parallel to uniform flow
$\bar{c}$: reference chord length
H : semi-height of tunnel transformed by Eq.(4)
L : semi-breadth of tunnel transformed by Eq.(4)
M : uniform stream Mach number
n : outward coordinate normal to boundary surface
R : downstream limit of x-coordinate of tunnel transformed by Eq.(4)
R^3 : three-dimensional Euclidean space
$\tilde{R}^3$: R^3 except S_w plane
$S(x,y)$: wing thickness distribution function transformed by Eq.(4)
S_{wing}: wing planform domain
S_{wake}: wake planform domain
S_w : sum of S_{wing} and S_{wake}
$S_2(x)$: airfoil thickness distribution function transformed by Eq.(4)
U_∞ : uniform stream speed
$U_{\infty c}$: corrected uniform stream speed
(u,v,w): (ϕ_x,ϕ_y,ϕ_z)
w_i : tunnel induced vertical velocity
$\hat{x}$: distance downstream (Origin is shown in Fig.1.)
$\hat{x}_L$: x-coordinate of wing leading edge
$\hat{x}_T$: x-coordinate of wing trailing edge
$\hat{y}$: spanwise distance normal to x-axis
$\hat{z}$: distance upwards from x-axis
(x,y,z): transformed coordinates by Eq.(4)
(ξ,η,ζ): (x,y,z)
$\alpha(\hat{y})$: incidence of airfoil section in yz-plane in a tunnel
$\tilde{\alpha}(\hat{y})$: incidence of airfoil section in yz-plane in free air
$\gamma_c(\hat{y})$: maximum camber of airfoil in yz-plane in a tunnel
$\tilde{\gamma}_c(\hat{y})$: maximum camber of airfoil in yz-plane in free air
λ : $= H/L$
Φ : full velocity potential
$\hat{\phi}$: small perturbation velocity potential in a tunnel
ϕ : transformed $\hat{\phi}$ by Eq.(4)
$\tilde{\phi}$: transformed small perturbation potential in free air by the same transformation to Eq.(4)
$\tilde{\Omega}$: Ω except S_w plane
Ω : $\{(x,y,z); |x|\leq R, |y|\leq L, |z|\leq H\}$
$\partial\tilde{\Omega}$: boundary surface of $\tilde{\Omega}$
$1(x)$: unit step function $\begin{cases} 1 & \text{for } x>0 \\ 0 & \text{for } x<0 \end{cases}$
$sgn(x)$: signal function $\begin{cases} 1 & \text{for } x>0 \\ -1 & \text{for } x<0 \end{cases}$

Subscripts and others

$_\infty$: denotes value of undisturbed stream
$\bar{(\ )}$: denotes average value
$\simeq$: denotes approximately equal relation
$\sum\sum'_{(m,n)}$: denotes that (n,m) takes all possible integral pairs except $(0,0)$

II. Wind Tunnel Wall Interference

Following three fundamental assumptions are adopted in this paper:

(1) Flow is inviscid and irrotaional.
(2) Wing is so thin that "thin wing approximation" may be applicable.
(3) Flow is subsonic everywhere.

Fundamental Equations

On the assumptions (1) to (3), the flow field equation is

$$\beta^2\frac{\partial^2\hat{\phi}}{\partial\hat{x}^2}+\frac{\partial^2\hat{\phi}}{\partial\hat{y}^2}+\frac{\partial^2\hat{\phi}}{\partial\hat{z}^2}=0, \qquad (1)$$

where $\beta=\sqrt{1-M^2}$, (2)

and the small perturbation velocity potential $\hat{\phi}$ has been defined as follows:

$$\Phi = U_\infty(x+\phi). \qquad (3)$$

Transforming $\hat{\phi}$ and $(\hat{x},\hat{y},\hat{z})$ by following equations:

$$\begin{cases} \phi = \beta^2\cdot\hat{\phi}, \\ (x,y,z) = (\hat{x},\beta\hat{y},\beta\hat{z}), \end{cases} \qquad (4)$$

we obtain

$$\Delta\phi = 0, \tag{5}$$

where

$$\Delta = \frac{\partial^2}{\partial\hat{x}^2}+\frac{\partial^2}{\partial\hat{y}^2}+\frac{\partial^2}{\partial\hat{z}^2}\ . \tag{6}$$

Boundary Value Problem

A function $\psi(\xi,\eta,\zeta;x,y,z)$ is introduced here which satisfies the following equation:

$$\Delta\psi = \delta(\xi,\eta,\zeta;x,y,z) \quad in\ \tilde{\Omega}\ , \tag{7}$$

where δ denotes the δ-function defined in $\tilde{\Omega}$ as shown in Fig.2. Using the Green's Formula and Eqs. (5) and (7), we obtain

$$\phi = \iint_{\partial\tilde{\Omega}}\left(\phi\frac{\partial\psi}{\partial n}-\psi\frac{\partial\phi}{\partial n}\right)dS. \tag{8}$$

After Eq.(8) is rearrenged on the second fundamental assumption, the upstream and downstream boundary surfaces normal to x-axis are displaced to infinity, that is, $R\to\infty$. Then Eq.(8) is reduced to

$$\begin{aligned}\phi =& -\iint_Y\{ug+v\psi\}_{-L}^{L}d\xi d\zeta\\ &-\iint_Z[uh+w\psi]_{-H}^{H}d\xi d\eta\\ &-\iint_{S_{wing}}S(\xi,\eta)\cdot\psi_\xi|_{\zeta=0}d\xi d\eta\\ &-\iint_{S_w}[\phi]_-^+\cdot\psi_\zeta|_{\zeta=0}d\xi d\eta,\end{aligned} \tag{9}$$

where

$$\iint_Y d\xi d\zeta = \int_{-\infty}^{\infty}d\xi\int_{-H}^{H}d\zeta, \tag{10}$$

$$\iint_Z d\xi d\eta = \int_{-\infty}^{\infty}d\xi\int_{-L}^{L}d\eta, \tag{11}$$

$$g = -\int_{\xi}^{\infty}\frac{\partial\psi}{\partial\eta}d\xi, \tag{12}$$

$$h = -\int_{\xi}^{\infty}\frac{\partial\psi}{\partial\zeta}d\xi, \tag{13}$$

$$\{H(\xi,\eta,\zeta)\}_{-L}^{L} = H(\xi,L,\zeta)-H(\xi,-L,\zeta), \tag{14}$$

$$[H(\xi,\eta,\zeta)]_{-H}^{H} = H(\xi,\eta,H)-H(\xi,\eta,-H), \tag{15}$$

$$[H(\xi,\eta,\zeta)]_-^+ = \lim_{\zeta\to0+}\{H(\xi,\eta,\zeta)-H(\xi,\eta,-\zeta)\}. \tag{16}$$

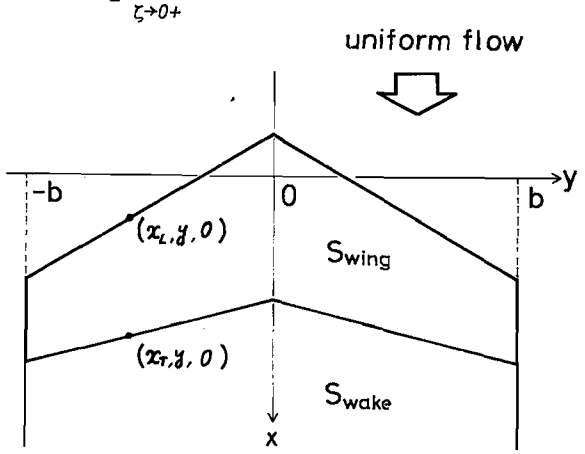

Fig.1 Wing Planform

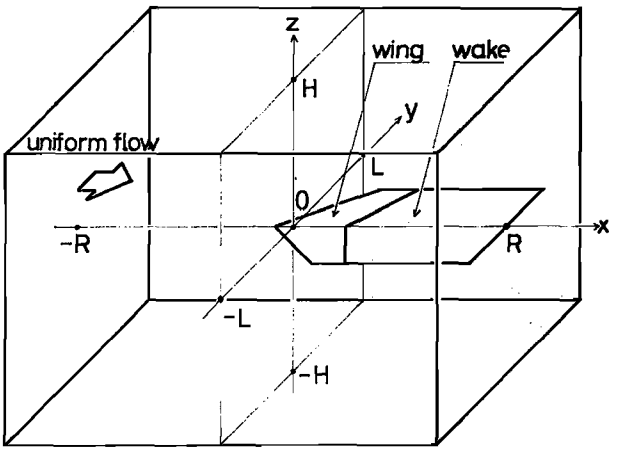

Fig.2 $\tilde{\Omega}$-Domain

In the same way, the following equation for $\tilde{\phi}$ in free air is obtained:

$$\begin{aligned}\tilde{\phi} =& -\iint_{S_{wing}}S(\xi,\eta)\cdot\tilde{\psi}_\xi|_{\zeta=0}d\xi d\eta\\ &-\iint_{S_w}[\tilde{\phi}]_-^+\cdot\tilde{\psi}_\zeta|_{\zeta=0}d\xi d\eta,\end{aligned} \tag{17}$$

where $\tilde{\psi}(\xi,\eta,\zeta;x,y,z)$ is a function which satisfies the following equation:

$$\Delta\tilde{\psi} = \delta(\xi,\eta,\zeta;x,y,z) \quad in\ \tilde{R}^3, \tag{18}$$

where δ denotes the δ-function defined in $\tilde{R}^3$. Because $[\phi]_-^+$ and $[\tilde{\phi}]_-^+$ on S_w are determined from the load distributions on S_{wing}, ϕ and $\tilde{\phi}$ can be estimated by the aid of Eqs.(9) and (17) respectively from the boundary values and their derivatives.

It should be noticed here that the following parts of the boundary surface $\partial\tilde{\Omega}$,

$$\Sigma_H = \{(x,y,H);x\in(-\infty,\infty),|y|\leq L\}, \tag{19}$$

$$\Sigma_{-H} = \{(x,y,-H);x\in(-\infty,\infty),|y|\leq L\}, \tag{20}$$

$$\Sigma_L = \{(x,L,z);x\in(-\infty,\infty),|z|\leq H\}, \tag{21}$$

and

$$\Sigma_{-L} = \{(x,-L,z);x\in(-\infty,\infty),|z|\leq H\} \tag{22}$$

are control surfaces. They must arround a wing model and be surrounded with the test section walls. Provided that these conditions are satisfied, L and H as well as the sectional shape of the test section are all arbitrary. Naturally, in the case of a rectangular test section, the walls can be regarded as the control surfaces if the existence of boundary layers on the walls is neglected. Hence, these control surfaces are called "wind tunnel walls" with the understanding stated above. Hereafter, only rectangular test sections will be considered.

Wind tunnel Wall Interference Potential

By the aid of Eq.(9), the small perturbation potential $\phi(x,y,z)$ can be estimated provided that

velocity components at the wind tunnel walls, Σ_H, Σ_{-H}, Σ_L and Σ_{-L} and $S(x,y)$ and $[\phi]^+_-$ distributions on S_{wing} are given. It should be noticed here that the pressure distribution on a wing installed in a wind tunnel as well as the shape and attitude of it cannot be determined uniquely only by the prescribing uniform flow conditions, wing planform, and thickness and load distributions on the wing. In addition to these conditions, velocity distributions on the tunnel walls must be known.

All wind tunnel tests presuppose that the load distribution on a wing in a tunnel should almost agree with that on the same wing in free air if the wing attitude and uniform stream conditions are slightly changed. We shall base on a similar premise in this paper: there are two wings which have the same planform and thickness distribution. One is in a tunnel and the other is in free air. On these conditions it is assumed that the two wings could have the same load distribution, but there would be differences in attitude and shape and pressure between the two in general. These differences are considered to be associated with wind tunnel wall interference. Then the following conditions are necessary in order to compare the perturbation potential in a tunnel with one in free air:

1°. Uniform stream conditions, M_∞, p_∞ (pressure), ρ_∞ (density), are the same.

2°. Wing planform S_{wing} is the same.

3°. Thickness distribution $S(x,y)$ is the same.

4°. Load distribution is the same.

On these conditions, wind tunnel wall interference potential φ is defined as follows:

$$\varphi(x,y,z) = \tilde{\phi}(x,y,z) - \phi(x,y,z). \qquad (23)$$

Because of the conditions 2° and 4°, there is no difference in $[\phi]^+_-$ distribution on S_w, that is,

$$[\phi]^+_- = [\tilde{\phi}]^+_- \quad \text{on } S_w . \qquad (24)$$

Then substituting Eqs.(8) and (17) in Eq.(23), we obtain

$$\begin{aligned}\varphi(x,y,z) = &\iint_{S_{wing}} S(\xi,\eta)\cdot(\psi_\xi|_{\zeta=0} - \tilde{\psi}_\xi|_{\zeta=0})\,d\xi d\eta \\ &+\iint_{S_w} [\phi]^+_-\cdot(\psi_\zeta|_{\zeta=0} - \tilde{\psi}_\zeta|_{\zeta=0})\,d\xi d\eta \\ &+\iint_Y \{ug + v\psi\}^L_{-L} d\xi d\zeta \\ &+\iint_Z [uh + w\psi]^H_{-H} d\xi d\eta. \qquad (25)\end{aligned}$$

In the right hand side of the above equation, all of g, h, ψ, $\psi_\xi|_{\zeta=0}$, $\tilde{\psi}_\xi|_{\zeta=0}$, $\psi_\zeta|_{\zeta=0}$, and $\tilde{\psi}_\zeta|_{\zeta=0}$ can be obtained analytically, and $S(x,y)$, $[\phi]^+_-$, $u|_{\eta=\pm L}$, $v|_{\eta=\pm L}$, $u|_{\zeta=\pm H}$, and $w|_{\zeta=\pm H}$ are all measurable in a wind tunnel test. So the wall interference potential $\varphi(x,y,z)$ can be determined completely. But it should be noticed that the 1st and 2nd partial derivatives of φ with respect to x, y and z on wing surface are necessary for wall interference correction. Hence, only those derivatives will be discussed hereafter.

Corrections for Wall Interference

Because the wing surface is regarded as coinciding with $z=0$ plane in the thin wing approximation, the values of derivatives of φ on wing surface is equivalent to those for z tending to zero from positive and negative sides. From the conditions 3° and 4°, the following equations are obtained:

$$\left.\frac{\partial\varphi}{\partial z}\right|_{z\to 0+} = \left.\frac{\partial\varphi}{\partial z}\right|_{z\to 0-}, \qquad (26)$$

$$\left.\frac{\partial\varphi}{\partial x}\right|_{z\to 0+} = \left.\frac{\partial\varphi}{\partial x}\right|_{z\to 0-}. \qquad (27)$$

From Eq.(26),

$$\tilde{\gamma}(\hat{y}) \simeq \alpha(\hat{y}) - \frac{1}{\beta}\{\varphi_z(0,0,\pm 0) + \frac{1}{2}(\hat{x}_L + \hat{x}_T)\cdot\varphi_{zx}(0,0,\pm 0) + \frac{1}{\beta}\varphi_{zy}(0,0,\pm 0)\cdot\hat{y}\}, \qquad (28)$$

where $\varphi_z(x,y,\pm 0)$ has been approximated by a polynomial of x and y of the first degree. In the same way, the maximum camber at $\hat{y}$ in free air can be estimated approximately by the following equation:

$$\tilde{\gamma}_c(\hat{y}) \simeq \gamma_c(\hat{y}) - \frac{1}{8\beta}\varphi_{zx}(0,0,\pm 0)\cdot c(\hat{y}), \qquad (29)$$

From Eq.(27), and by the aid of the small perturbation potential theory, the static pressure coefficient on a wing in free air is obtained as follows:

$$\tilde{C}_p(\hat{x},\hat{y}) = C_p(\hat{x},\hat{y}) - \frac{2}{\beta^2}\cdot\varphi_x(\hat{x},\beta\hat{y},\pm 0). \qquad (30)$$

By the aid of Eqs.(28) to (30), the wing shape and attitude and the static pressure distribution on the wing surface in free air can be determined uniquely from the values obtained in a wind tunnel test. However, the wing drag in free air is different from that in a tunnel because the pressure distributions on the two wings are different. It is often the most important purpose of wind tunnel tests to estimate the drag in free air. Therefore, wind tunnel tests almost lose their value if the measured drag is of no use. Hence it is assumed here that the same wing surface pressure as in a tunnel should exist in free air at some speed $U_{\infty C}$ slightly different from U_∞, that is,

$$U_{\infty C} = U_\infty\left(1 - \frac{1}{\beta^2}\bar{\varphi}_x\right|_{z\to\pm 0}), \qquad (31)$$

where

$$\bar{\varphi}_x\Big|_{z\to\pm 0} = \frac{1}{A}\iint_{S_{wing}} \varphi_x\Big|_{z\to\pm 0} dxdy. \qquad (32)$$

Then the model drag in free air is the same with that in a tunnel. But uniform stream Mach number and uniform stream dynamic pressure in free air with uniform speed $U_{\infty C}$ are slightly changed because uniform stream conditions in free air are different from those in a tunnel. Corrections to these quantities can be estimated by means of blockage factor ε_B defined as follows:

$$\varepsilon_B = -\frac{1}{\beta^2}\bar{\varphi}_x\Big|_{z\to\pm 0} . \qquad (33)$$

Ref.(14) details formulae for those values.

ψ and $\breve{\psi}$

The solutions of Eqs.(7) and (18) are

$$\psi(\xi,\eta,\zeta;x,y,z)$$
$$= \frac{1}{8HL}|\xi-x| - \frac{1}{4\pi H}\sum_{m=1}^{\infty}\frac{1}{m}\cdot\exp\left(-\frac{m\pi}{L}|\xi-x|\right)\cos\frac{m\pi}{L}(\eta-y)$$
$$-\frac{1}{4\pi L}\sum_{n=1}^{\infty}\frac{1}{n}\exp\left(-\frac{n\pi}{H}|\xi-x|\right)\cos\frac{n\pi}{H}(\zeta-z)$$
$$-\frac{1}{2HL}\sum_{n=1}^{\infty}\sum_{m=1}^{\infty}\frac{1}{k}\exp(k|\xi-x|)\cos\frac{m\pi}{L}(\eta-y)\cos\frac{n\pi}{H}(\zeta-z), \qquad (34)$$

and

$$\breve{\psi}(\xi,\eta,\zeta;x,y,z) = -\frac{1}{4\pi}\{(\xi-x)^2+(\eta-y)^2+(\zeta-z)^2\}^{-1/2}, \qquad (35)$$

where

$$k = \pi\sqrt{\left(\frac{n}{H}\right)^2+\left(\frac{m}{L}\right)^2} . \qquad (36)$$

III. Blockage Effect

As was mentioned in the previous section, $\varphi_x(x, y,\pm 0)$ must be known in order to assess the blockage effect. It can be approximated by $\varphi_x(0,0,\pm 0)$ because reference chord length $\bar{c}$ and wing span $2b$ are usually small compared with the height and breadth of tunnel respectively. Then,

$$\varepsilon_B \simeq -\frac{1}{\beta^2}\varphi_x(0,0,\pm 0). \qquad (37)$$

In this section, only $\varphi_x(0,0,\pm 0)$ is estimated. $\varphi_x(x,y,\pm 0)$ can be estimated in the same way but with a little more difficulty.

Blockage Factor

From Eq.(25), we obtain

$$\varphi_x(0,0,\pm 0)$$
$$= \iint_{S_{wing}} S(\xi,\eta)\frac{\partial}{\partial x}\left\{\frac{\partial\psi}{\partial\xi}\Big|_{\zeta=0} - \frac{\partial\breve{\psi}}{\partial\xi}\Big|_{\zeta=0}\right\}_{\substack{x=y=0\\ z\to\pm 0}} d\xi d\eta$$
$$+2\iint_{Y}\psi_x(\xi,L,\zeta;0,0,\pm 0)\cdot v_L^a(\xi,\zeta)d\xi d\zeta$$
$$+2\iint_{Z}\psi_x(\xi,\eta,H;0,0,\pm 0)\cdot w_H^a(\xi,\eta)d\xi d\eta, \qquad (38)$$

where

$$v_L^a(\xi,\zeta) = \frac{1}{2}\{v(\xi,\eta,\zeta)\}_{-L}^{L} , \qquad (39)$$

$$w_H^a(\xi,\eta) = \frac{1}{2}[w(\xi,\eta,\zeta)]_{-H}^{H} . \qquad (40)$$

From Eqs.(34) and (35),

$$\left(\frac{\partial}{\partial x}\left\{\frac{\partial\psi}{\partial\xi}\Big|_{\zeta=0} - \frac{\partial\breve{\psi}}{\partial\xi}\Big|_{\zeta=0}\right\}\right)_{\substack{x=y=0\\ z\to\pm 0}}$$
$$= -\frac{1}{4\pi}\sum_{(m,n)}'\left\{\frac{1}{W_{m,n}^3} - 3\frac{(\xi-x)^2}{W_{m,n}^5}\right\}\Big|_{\substack{x=y=0\\ z\to\pm 0}} , \qquad (41)$$

where

$$W_{m,n}(\xi,\eta;x,y,z) = \sqrt{(\xi-x)^2+(2Lm+\eta-y)^2+(2Hn+z)^2} . \qquad (42)$$

And from Eq.(34),

$$\psi_x(\xi,L,\zeta;0,0,\pm 0)$$
$$= -\frac{1}{8HL}\tanh\left(\frac{\pi}{2}\cdot\frac{\xi}{L}\right) - \frac{1}{H^2}\cdot\frac{\xi}{L}\sum_{n=1}^{\infty}\sum_{\nu=1}^{\infty}\frac{n}{\sqrt{(2\nu-1)^2+(\xi/L)^2}}$$
$$\times K_1\left(\frac{n\pi}{\lambda}\sqrt{(2\nu-1)^2+(\xi/L)^2}\right)\cos\frac{n\pi}{H}\zeta, \qquad (43)$$

and

$$\psi_x(\xi,\eta,H;0,0,\pm 0)$$
$$= -\frac{1}{8HL}\tanh\left(\frac{\pi}{2}\cdot\frac{\xi}{H}\right) - \frac{1}{L^2}\cdot\frac{\xi}{H}\sum_{m=1}^{\infty}\sum_{\nu=1}^{\infty}\frac{m}{\sqrt{(2\nu-1)^2+(\xi/H)^2}}$$
$$\times K_1\left(m\pi\lambda\sqrt{(2\nu-1)^2+(\xi/H)^2}\right)\cos\frac{m\pi}{L}\eta , \qquad (44)$$

where

$$K_1(x) = \frac{1}{x} + \sum_{\nu=0}^{\infty}\frac{(x/2)^{2\nu+1}}{\nu!(\nu+1)!}\left\{\ln\frac{x}{2} - \psi(\nu+1) - \frac{1}{2(\nu+1)}\right\}, x>0, \qquad (45)$$

$$\psi(\nu+1) = \sum_{r=1}^{\nu}\frac{1}{r} - \gamma, \quad \psi(1) = -\gamma, \qquad (46)$$

$$\gamma = \lim_{n\to\infty}\left(1+\frac{1}{2}+\frac{1}{3}+\cdots+\frac{1}{n}-\ln(n)\right). \qquad (47)$$

$K_1(x)$ decreases with x as rapidly as an exponential function does. For example, $K_1(9\pi)$ is as small as 1.369×10^{-13}.

If tunnel walls are solid, the following conditions are obtained:

$$v_L^a(\xi,\zeta) = w_H^a(\xi,\eta) = 0. \qquad (48)$$

Using a new notation φ_x^s for $\varphi_x(0,0,\pm 0)$ in the above conditions, we obtain from Eq.(25)

$$\varphi_x^s = \iint_{S_{wing}} S(\xi,\eta)\frac{\partial}{\partial x}\left\{\frac{\partial\psi}{\partial\xi}\Big|_{\zeta=0} - \frac{\partial\breve{\psi}}{\partial\xi}\Big|_{\zeta=0}\right\}_{\substack{x=y=0\\ z\to\pm 0}} d\xi d\eta. \qquad (49)$$

For a small wing model with volume V, $S(x,y)$ can be expressed approximately by the following expression:

$$S(x,y) = \beta^2 V\delta(x,y), \qquad (50)$$

where δ denotes δ-function on S_{wing}. Substituting Eq.(50) for $S(\xi,\eta)$ in Eq.(49), we obtain

$$\frac{\varepsilon_B}{V}=\frac{1}{16\pi}\left(\frac{1}{L^3}+\frac{1}{H^3}\right)\sum_{n=1}^{\infty}\frac{1}{n^3}+\frac{1}{8\pi}\sum_{n=1}^{\infty}\sum_{m=1}^{\infty}\frac{1}{\sqrt{(nH)^2+(mL)^2}^3}. \quad (51)$$

This expression is identical with Eq.(5.22) of Ref. (14). Eq.(41) behaves as a weight function for $S(x, y)$ and it gives useful information about the limitation on dimensions of a wing model. In Fig.3, the dimensionless weight functions multiplied by $(HL)^{3/2}$ are contoured only in the region where both ξ and η are non-negative because they are symmetric with respect to both ξ and η.

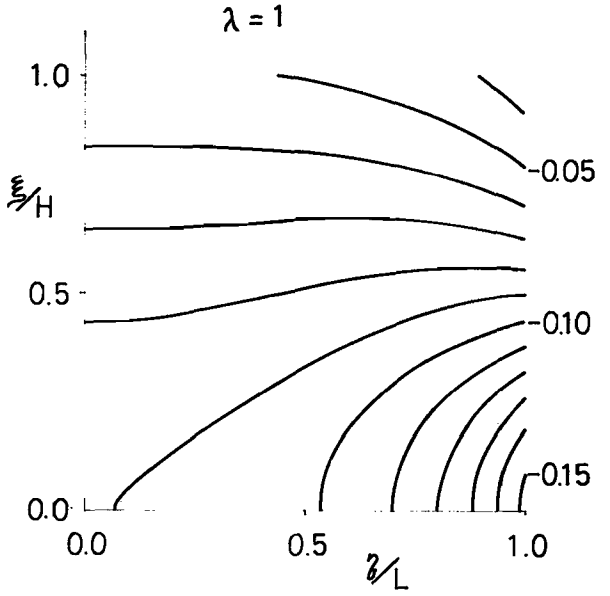

Fig.3-1 Weight Function for $S(\xi,\eta)$, $(\lambda=1)$

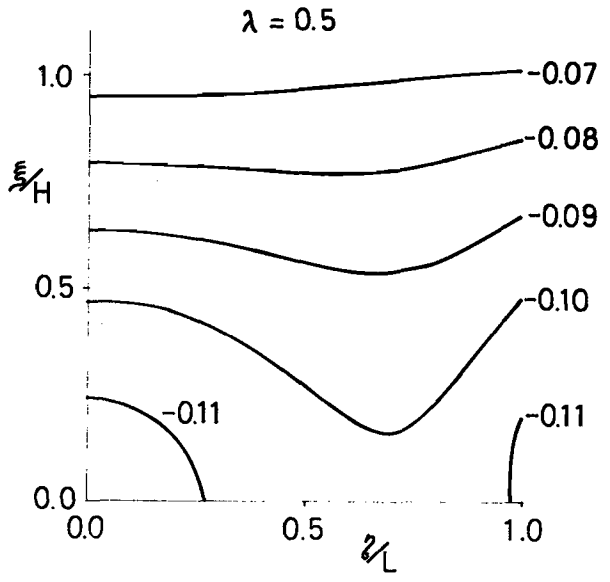

Fig.3-2 Weight Function for $S(\xi,\eta)$, $(\lambda=0.5)$

More Convenient Method

It seems very difficult to measure the distributions of $v_L^a(\xi,\zeta)$ and $w_H^a(\xi,\eta)$ over the whole boundary walls of test section. They change, however, only gradually on the walls standing sufficiently far from a wing model which is the disturbance source. Then if these distributions are expanded in the following Fourier serieses of ζ and η respectively, we have

$$v_L^a(\xi,\zeta)=\frac{1}{2}v_{Lc}^{a(0)}+\sum_{n=1}^{\infty}\left\{v_{Ls}^{a(n)}\cdot\sin\frac{n\pi}{H}\zeta+v_{Lc}^{a(n)}\cdot\cos\frac{n\pi}{H}\zeta\right\}, \quad (52)$$

$$w_H^a(\xi,\eta)=\frac{1}{2}w_{Hc}^{a(0)}+\sum_{m=1}^{\infty}\left\{w_{Hs}^{a(m)}\cdot\sin\frac{m\pi}{L}\eta+w_{Hc}^{a(m)}\cdot\cos\frac{m\pi}{L}\eta\right\}, \quad (53)$$

where

$$v_{Lc}^{a(n)}(\xi)=\frac{1}{H}\int_{-H}^{H}v_L^a(\xi,\zeta)\cos\frac{n\pi}{H}\zeta\,d\zeta, \quad (n=0,1,2,\ldots), \quad (54)$$

$$v_{Ls}^{a(n)}(\xi)=\frac{1}{H}\int_{-H}^{H}v_L^a(\xi,\zeta)\sin\frac{n\pi}{H}\zeta\,d\zeta, \quad (n=1,2,3,\ldots), \quad (55)$$

$$w_{Hc}^{a(m)}(\xi)=\frac{1}{L}\int_{-L}^{L}w_H^a(\xi,\eta)\cos\frac{m\pi}{L}\eta\,d\eta, \quad (m=0,1,2,\ldots), \quad (56)$$

$$w_{Hs}^{a(m)}(\xi)=\frac{1}{L}\int_{-L}^{L}w_H^a(\xi,\eta)\sin\frac{m\pi}{L}\eta\,d\eta, \quad (m=1,2,3,\ldots). \quad (57)$$

Fig.4 shows $v_{Lc}^{a(n)}$ and $w_{Hc}^{a(m)}$ for $m,n = 0,1$.

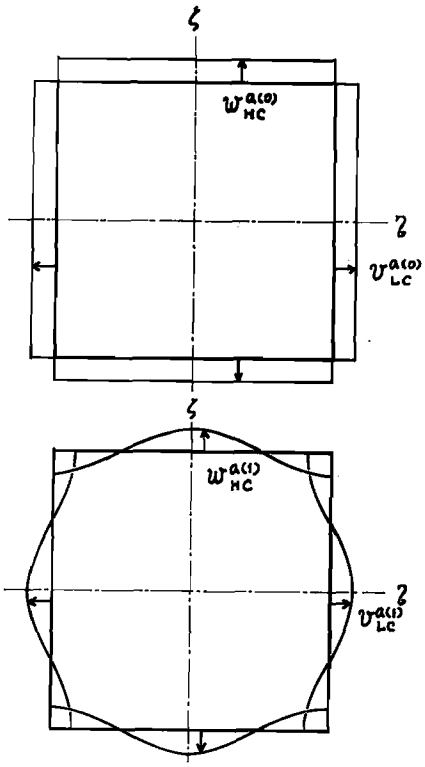

Fig.4 $v_{Lc}^{a(n)}$ and $w_{Hc}^{a(m)}$, $(m,n=0,1)$

We assume that the higher harmonic terms in Eqs. (52) and(53) are negligible, so

$$v_{Lc}^{a(n)}(\xi) = v_{Ls}^{a(n)}(\xi) = 0 \quad \text{for } n > N_B, \qquad (58)$$

$$w_{Hc}^{a(m)}(\xi) = w_{Hs}^{a(m)}(\xi) = 0 \quad \text{for } m > M_B, \qquad (59)$$

where N_B and M_B are integers. On the above assumptions, Eq.(38) is reduced to

$$\begin{aligned}
&\varphi_x(0,0,\pm 0) \\
&= \varphi_x^s - \int_{-\infty}^{\infty} v_{Lc}^{a(0)}(\xi)\cdot\frac{1}{4}\tanh\left(\frac{\pi}{2}\cdot\frac{\xi}{L}\right)d\left(\frac{\xi}{L}\right) \\
&- \sum_{n=1}^{N_B}\int_{-\infty}^{\infty} v_{Lc}^{a(n)}(\xi)\cdot\frac{2n}{\lambda}\sum_{\nu=1}^{\infty}\frac{(\xi/L)}{\sqrt{(2\nu-1)^2+(\xi/L)^2}} \\
&\times K_1\left(\frac{n\pi}{\lambda}\sqrt{(2\nu-1)^2+(\xi/L)^2}\right)d\left(\frac{\xi}{L}\right) \\
&- \int_{-\infty}^{\infty} w_{Hc}^{a(0)}(\xi)\cdot\frac{1}{4}\tanh\left(\frac{\pi}{2}\cdot\frac{\xi}{H}\right)d\left(\frac{\xi}{H}\right) \\
&- \sum_{m=1}^{M_B}\int_{-\infty}^{\infty} w_{Hc}^{a(m)}(\xi)\cdot 2m\lambda\sum_{\nu=1}^{\infty}\frac{(\xi/H)}{\sqrt{(2\nu-1)^2+(\xi/H)^2}} \\
&\times K_1\left(m\pi\lambda\sqrt{(2\nu-1)^2+(\xi/H)^2}\right)d\left(\frac{\xi}{H}\right). \qquad (60)
\end{aligned}$$

Figs.5-1 and 5-2 show weight functions for $v_{Lc}^{a(n)}$ in Eq.(60), that is,

$$\frac{1}{4}\cdot\tanh\left(\frac{\pi}{2}\cdot\frac{\xi}{L}\right),$$

$$\frac{2n}{\lambda}\sum_{\nu=1}^{\infty}\frac{\xi/L}{\sqrt{(2\nu-1)^2+(\xi/L)^2}}\cdot K_1\left(\frac{n\pi}{\lambda}\sqrt{(2\nu-1)^2+(\xi/L)^2}\right).$$

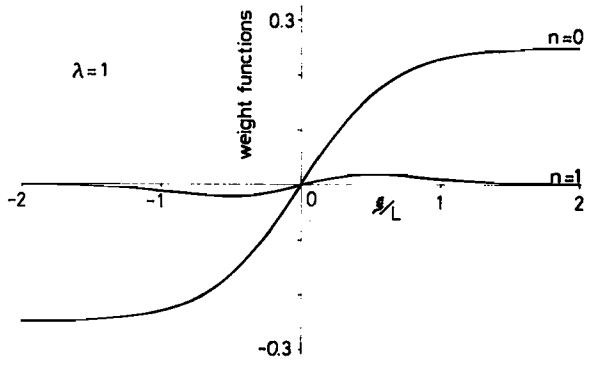

Fig.5-1 Weight Functions for $v_{Lc}^{a(n)}$ (n=0,1)

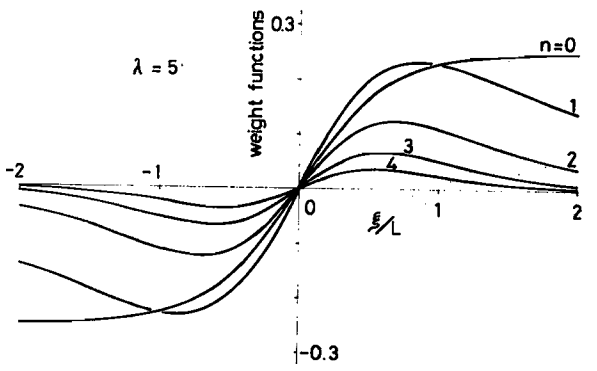

Fig.5-2 Weight Functions for $v_{Lc}^{a(n)}$ (n=0,1,2,3,4)

Weight functions for $w_{Hc}^{a(m)}$ are the same to those for $v_{Lc}^{a(n)}$ if ξ/H and $m\lambda$ are substituted for ξ/L and n/λ respectively. Then only the weight functions for $v_{Lc}^{a(n)}$ are shown. Weight functions for higher harmonics of $v_{Lc}^{a(n)}$ and $w_{Hc}^{a(m)}$ vanish rapidly with n and m as can be seen in Figs.5-1 and 5-2. Moreover, higher harmonics of $v_{Lc}^{a(n)}$ and $w_{Hc}^{a(m)}$ are also small in magnitude. So these higher harmonic terms have almost no effect on blockage interference except that λ is very large or small. In the case of two-dimensional tunnel, λ usually ranges from 3 to 5. Then $v_{Lc}^{a(1)}$ and $v_{Lc}^{a(2)}$ may have a rather large effect on the blockage interference.

Rectangular Test Section with Solid Side Walls

Provided that the two side walls are solid and that a model and the flow field disturbed by it are symmetric with respect to xz-plane, w_H^a and v_L^a are uncoupled with each other. Then $w_H^a(x,y)$ can be obtained from measured static pressure distributions on the top and bottom walls. Because static pressure coefficient can be expressed easily by x-component of the small perturbation velocity, $\varphi_x(0,0,\pm 0)$ is reduced to

$$\begin{aligned}
&\varphi_x(0,0,\pm 0) \\
&= \varphi_x^s - \int_{x_L}^{x_T} S_x^{(0)}\cdot\left\{\frac{1}{8}\tanh\left(\frac{\pi}{4}\cdot\frac{\xi}{H}\right)\right\}d\left(\frac{\xi}{H}\right) \\
&- \sum_{m=1}^{\infty}\int_{x_L}^{x_T} S_x^{(m)}\cdot J_1^{(m)}\left(\frac{\xi}{2H}\right)d\left(\frac{\xi}{H}\right) \\
&+ \int_{-\infty}^{\infty} u_{Hc}^{s(0)}\cdot\left\{-\frac{1}{4}\operatorname{sech}\left(\frac{\pi}{2}\cdot\frac{\xi}{H}\right)\right\}d\left(\frac{\xi}{H}\right) \\
&+ \sum_{m=1}^{\infty}\int_{-\infty}^{\infty} u_{Hc}^{s(m)}\cdot J_2^{(m)}\left(\frac{\xi}{H}\right)d\left(\frac{\xi}{H}\right), \qquad (61)
\end{aligned}$$

where

$$S_x^{(m)} = \frac{1}{L}\int_{-L}^{L}\frac{\partial S}{\partial\xi}\cdot\cos\frac{m\pi}{L}\eta\,d\eta, \quad (m=0,1,2,\ldots), \qquad (62)$$

$$u_{Hc}^{s(m)} = \frac{1}{L}\int_{-L}^{L} u_H^s(\xi,\eta)\cdot\cos\frac{m\pi}{L}\eta\,d\eta, \quad (m=0,1,2,\ldots), \qquad (63)$$

$$u_H^s(\xi,\eta) = \frac{1}{2}\{u(\xi,\eta,H) + u(\xi,\eta,-H)\}, \qquad (64)$$

$$J_1^{(m)}(x) = 2m\lambda\sum_{n=1}^{\infty}\frac{x}{\sqrt{(2n-1)^2+x^2}}K_1\left(2m\pi\lambda\sqrt{(2n-1)^2+x^2}\right), \qquad (65)$$

$$J_2^{(m)}(x) = 2m\lambda\sum_{n=1}^{\infty}\frac{(-1)^n(2n-1)}{\sqrt{(2n-1)^2+x^2}}K_1\left(m\pi\lambda\sqrt{(2n-1)^2+x^2}\right). \qquad (66)$$

As can be seen in Figs.6-1 and 6-2, higher harmonics of u_H^s have almost no effect on the blockage interference.

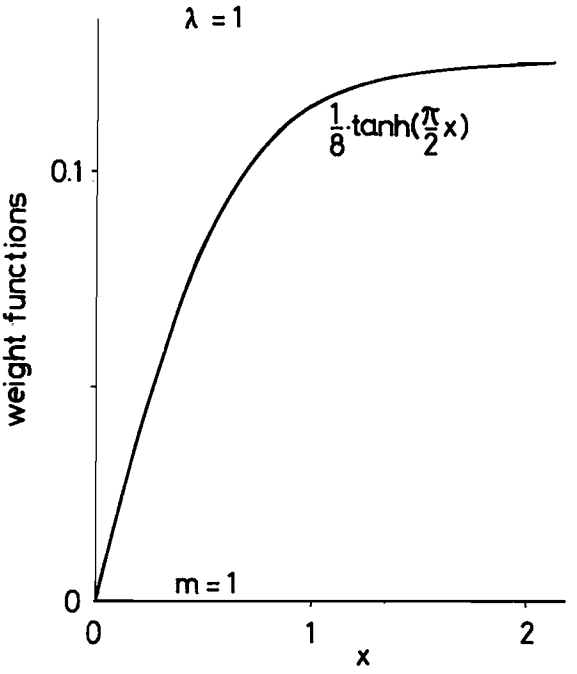

Fig.6-1 Weight Functions for $S_x^{(m)}$ $(m=0,1)$

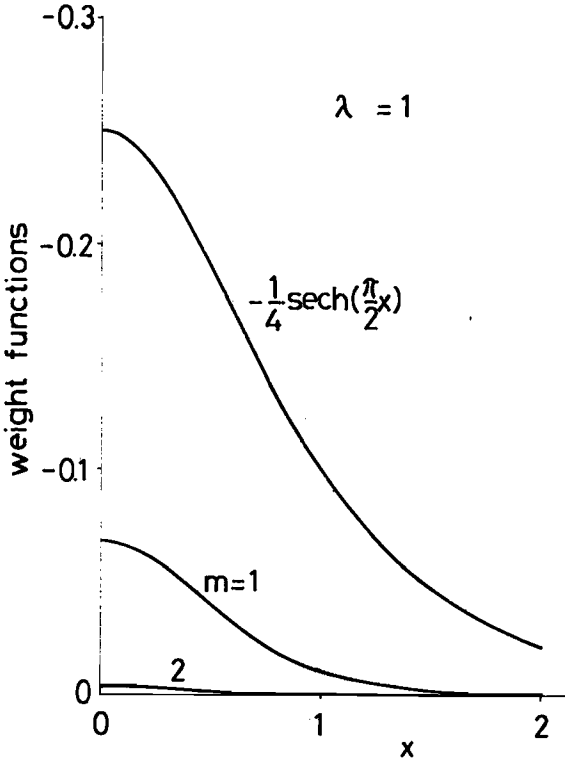

Fig.6-2 Weight Functions for $u_{Hc}^{s(m)}$ $(m=0,1,2)$

IV. Lift Interference Effect

As was mentioned in the previous section, $\varphi_z(x, y, \pm 0)$ must be known in order to estimate the lift interference effect. By the use of Eq.(28), however, the interference can be estimated with sufficient accuracy from $\varphi_z(0,0,\pm 0)$, $\varphi_{zx}(0,0,\pm 0)$ and $\varphi_{zy}(0,0,\pm 0)$. Only $\varphi_z(0,0,\pm 0)$ will be estimated in this section. In the same way, estimated are $\varphi_{zx}(0,0,\pm 0)$ easily, and $\varphi_{zy}(0,0,\pm 0)$ with a little more difficulty.

Lift Interference Parameter

From Eq.(25),

$$\varphi_z(0,0,\pm 0) = \iint_{S_w} [\phi]_-^+ \frac{\partial}{\partial z}\{\frac{\partial \psi}{\partial \zeta}\Big|_{\zeta=0} - \frac{\partial \bar{\psi}}{\partial \zeta}\Big|_{\zeta=0}\}_{\substack{x=y=0 \\ z\to\pm 0}} d\xi d\eta + 2\iint_Y \psi_z(\xi,L,\zeta;0,0,\pm 0)\cdot v_L^a(\xi,\zeta)\,d\xi d\zeta + 2\iint_Z h_z(\xi,\eta,H;0,0,\pm 0)\cdot u_H^a(\xi,\eta)\,d\xi d\eta, \quad (67)$$

where

$$u_H^a(\xi,\eta) = \frac{1}{2}[u(\xi,\eta,\zeta)]_{-H}^{H}. \quad (68)$$

We obtain from Eqs.(34) and (35)

$$\frac{\partial}{\partial z}\{\frac{\partial \psi}{\partial \zeta}\Big|_{\zeta=0} - \frac{\partial \bar{\psi}}{\partial \zeta}\Big|_{\zeta=0}\} = -\frac{1}{4\pi}\sum_{(m,n)}'\{\frac{1}{W_{m,n}^3} - 3\frac{(2Hn+z)^2}{W_{m,n}^5}\} \quad (69)$$

and also from Eqs.(13) and (34)

$$\psi_z(\xi,L,\zeta;0,0,\pm 0) = -\frac{1}{H^2}\sum_{n=1}^{\infty}\sum_{\nu=1}^{\infty} n\cdot K_0\{\frac{n\pi}{\lambda}\sqrt{(2\nu-1)^2+(\xi/L)^2}\}\sin\frac{n\pi}{H}\zeta, \quad (70)$$

$$h_z(\xi,\eta,H;0,0,\pm 0) = -\frac{1}{4HL}\cdot\frac{1}{1+\exp(\pi\xi/H)} + \lim_{z\to\pm 0}\frac{\pi^2}{2H^3L}\sum_{n=1}^{\infty}\sum_{m=1}^{\infty}(-1)^n\cdot\frac{n^2}{k^2}\times K(\xi;0;k)\cos\frac{m\pi}{L}\eta\cdot\cos\frac{n\pi}{H}z, \quad (71)$$

where

$$K(\xi;x;k) = \mathrm{sgn}(\xi-x)\cdot e^{-k|\xi-x|} + 2\cdot 1(x-\xi), \quad (72)$$

and $K_0(x)$ denotes a modified Bessel function:

$$K_0(x) = -\sum_{\nu=0}^{\infty}\{\frac{(x/2)^\nu}{\nu!}\}^2\{\ln\frac{x}{2} - \psi(\nu+1)\}, \quad (x>0). \quad (73)$$

$K_0(x)$ decreases as rapidly as $K_1(x)$ with x. For example, $K_0(9\pi)$ is as small as 1.345×10^{-13}.

If a lifting wing and its trailing edge vortices are modeled by a horse-shoe vortex as shown in Fig. 7, $[\phi]_-^+$ can be expressed as follows:

$$[\phi]_-^+ = \begin{cases} \Gamma\cdot\bar{c} & \text{for } |y| \le b \text{ and } x \in [0,\infty), \\ 0 & \text{otherwise.} \end{cases} \quad (74)$$

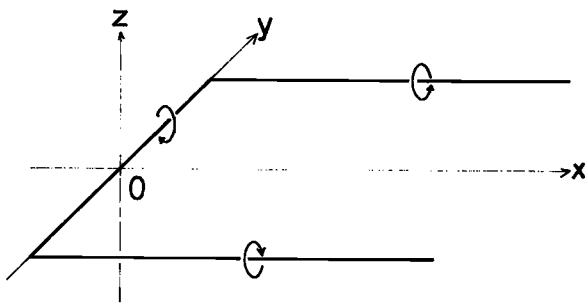

Fig.7 Horse-Shoe Vortex

Using a new notation φ_z^0 for $\varphi_z(0,0,\pm 0)$ in the case of the top and bottom walls open and the two side walls solid, we obtain

$$\varphi_z^0 = \Gamma\cdot\bar{c}\{\frac{b}{4HL} - \frac{1}{2L}\sum_{n=1}^{\infty}\frac{\pi^{2n-1}}{(2n)!}\cdot B_n\cdot\left(\frac{b}{L}\right)^{2n-1} + \frac{1}{2L}\sum_{m=1}^{\infty} e^{-m\pi\lambda}\cdot cosech(m\pi\lambda)\cdot\sin\frac{m\pi}{L}b\}, \quad (75)$$

because

$$v_L^a(\xi,\zeta) = u_H^a(\xi,\eta) = 0. \quad (76)$$

In general, the lift interference parameter is defined as follows[13]:

$$\delta_0 = \frac{Cw_i}{U_\infty AC_L}. \quad (77)$$

Substituting φ_z for w_i in Eq.(77), we obtain

$$\delta_0 = -\frac{HL}{b\Gamma\bar{c}}\cdot\varphi_z. \quad (78)$$

Denoting δ_0 corresponding to φ_z^0 by δ_0^0, we get from Eq.(75)

$$\delta_0^0 = -\frac{1}{4} + \frac{\lambda}{2}\sum_{n=1}^{\infty}\frac{\pi^{2n-1}}{(2n)!}\cdot B_n\cdot\left(\frac{b}{L}\right)^{2(n-1)} - \frac{L\lambda}{2b}\sum_{m=1}^{\infty} e^{-m\pi\lambda}\cdot cosech(m\pi\lambda)\sin\frac{m\pi}{L}b. \quad (79)$$

In the case of small lifting wing, that is, making b tend to zero while keeping $\Gamma\bar{c}$ finite, we obtain

$$\delta_0^0 = -\frac{1}{4} + \frac{\pi}{24}\lambda - \pi\lambda\sum_{m=1}^{\infty}\frac{m}{exp(2m\pi\lambda)-1}. \quad (80)$$

The above expression is identical with Eq.(3.17) in Ref.(13).

More Convenient Method

u_H^a can be expanded to the Fourier series with respect to η:

$$u_H^a(\xi,\eta) = \frac{1}{2}u_{Hc}^{a(0)} + \sum_{m=1}^{\infty}\{u_{Hs}^{a(m)}\cdot\sin\frac{m\pi}{L}\eta + u_{Hc}^{a(m)}\cdot\cos\frac{m\pi}{L}\eta\}, \quad (81)$$

where

$$u_{Hc}^{a(m)}(\xi) = \frac{1}{L}\int_{-L}^{L} u_H^a(\xi,\eta)\cdot\cos\frac{m\pi}{L}\eta d\eta, (m=0,1,2,\ldots), \quad (82)$$

$$u_{Hs}^{a(m)}(\xi) = \frac{1}{L}\int_{-L}^{L} u_H^a(\xi,\eta)\cdot\sin\frac{m\pi}{L}\eta d\eta, (m=1.2,3,\ldots). \quad (83)$$

For the same reason as was mentioned in the previous section III, higher harmonics of $u_{Hc}^{a(m)}$ and $u_{Hs}^{a(m)}$ can be negligible. So

$$u_{Hc}^{a(m)}(\xi) = u_{Hs}^{a(m)}(\xi) = 0 \quad for\ m > M_L. \quad (84)$$

It follows from Eqs.(58) and (84) that Eq.(67) is reduced to

$$\begin{aligned}\varphi_z(0,0,\pm 0) &= \varphi_z^0 - \sum_{n=1}^{N_B}\int_{-\infty}^{\infty} v_{Ls}^{a(n)}\frac{2n}{\lambda}\sum_{\nu=1}^{\infty}K_0\left(\frac{n\pi}{\lambda}\sqrt{(2\nu-1)^2+(\xi/L)^2}\right)d\left(\frac{\xi}{L}\right)\\ &-\int_{-\infty}^{\infty} u_{Hc}^{a(0)}\cdot\frac{1}{2}\cdot\frac{1}{1+exp(\pi\xi/H)}d\left(\frac{\xi}{H}\right)\\ &-\sum_{m=1}^{M_L}\int_{-\infty}^{\infty} u_{Hc}^{a(m)}\cdot\{\frac{m\pi\lambda}{2}cosech(m\pi\lambda)\cdot 1(-\xi)\\ &+\frac{1}{4}\cdot e^{-m\pi\lambda|\xi|/H}\cdot sgn(\xi)\\ &+(m\lambda)^2\cdot sgn(\xi)\sum_{n=1}^{\infty}\frac{(-1)^n}{n^2+(m\lambda)^2}e^{-\pi\sqrt{n^2+(m\lambda)^2}\frac{|\xi|}{H}}\\ &-m\lambda\frac{\xi}{H}\sum_{\nu=1}^{\infty}\frac{1}{\sqrt{(2\nu-1)^2+(\xi/L)^2}}\cdot K_1\left(m\pi\lambda\sqrt{(2\nu-1)^2+(\xi/H)^2}\right)d\left(\frac{\xi}{H}\right). \quad (85)\end{aligned}$$

Figs.8-1 and 8-2 show $v_{Ls}^{a(n)}$ and $u_{Hc}^{a(m)}$.

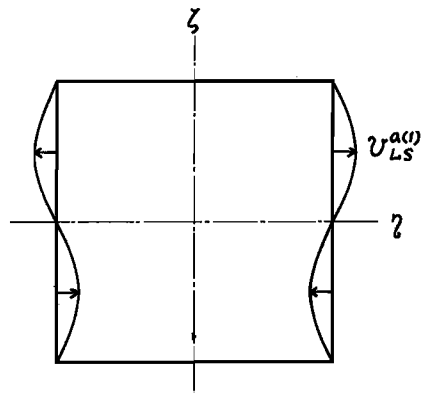

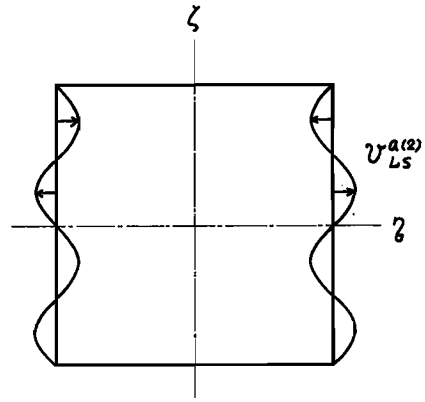

Fig.8-1 $v_{Ls}^{a(n)}$ (n=1,2)

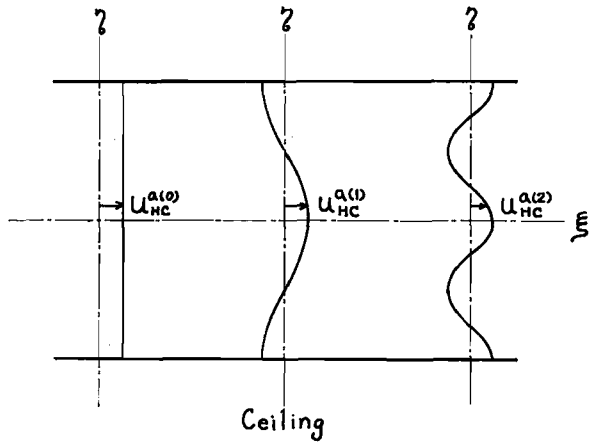

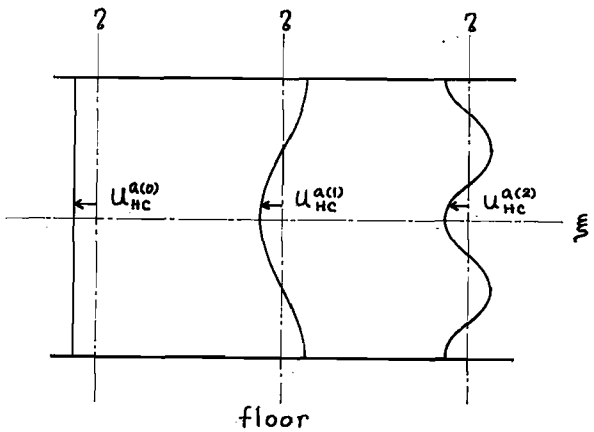

Fig.8-2 $u_{Hc}^{a(m)}$ $(m=0,1,2)$

Weight functions for $v_{Ls}^{a(n)}$ and $u_{Hc}^{a(m)}$ in Eq.(85), that is,

$$\frac{2\pi}{\lambda}\sum_{\nu=1}^{\infty} K_0\left(\frac{n\pi}{\lambda}\sqrt{(2\nu-1)^2+(\xi/L)^2}\right),$$

$$\frac{1}{2}\cdot\frac{1}{1+\exp(\pi\xi/H)}, \text{ etc.}$$

vanish rapidly with n and m increasing as can be seen in Figs.9 and 10.

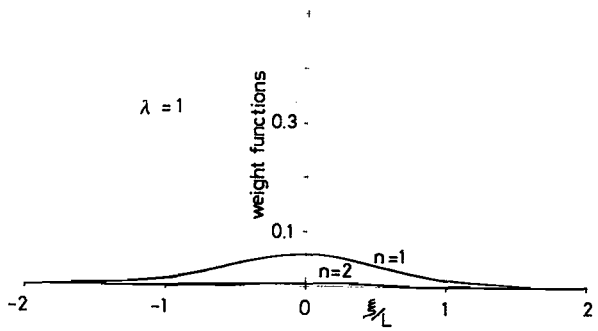

Fig.9-1 Weight Functions for $v_{Ls}^{a(n)}$ $(\lambda=1)$

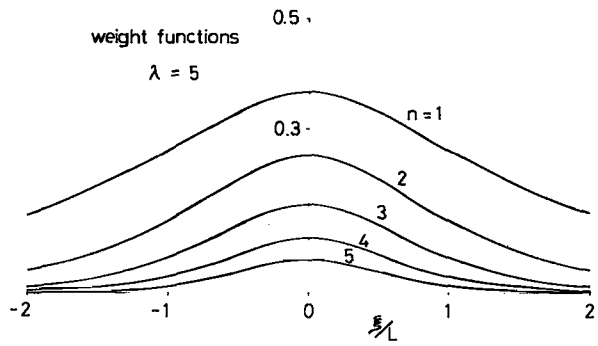

Fig.9-2 Weight Functions for $v_{Ls}^{a(n)}$ $(\lambda=5)$

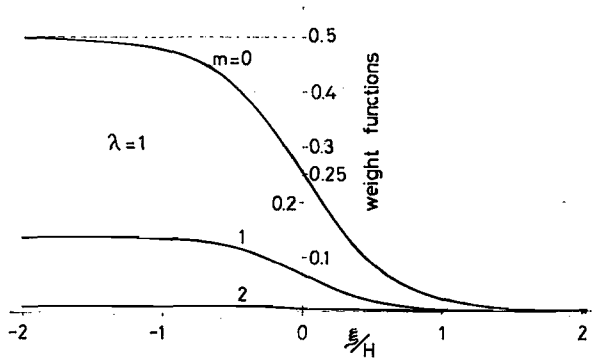

Fig.10-1 Weight Functions for $u_{Hc}^{a(m)}$ $(\lambda=1)$

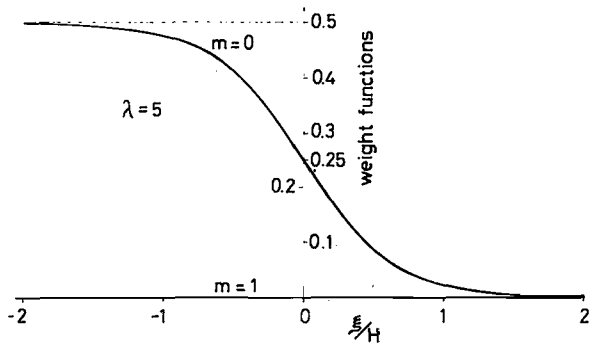

Fig.10-2 Weight Functions for $u_{Hc}^{a(m)}$ $(\lambda=5)$

The higher harmonics of $v_{Ls}^{a(n)}$ and $u_{Hc}^{a(m)}$ are small as well as their weight functions. So these higher harmonic terms have almost no effect on lift interference unless λ is very large or small. In the case of a two-dimensional tunnel, λ usually ranges from 3 to 5, then $v_{Ls}^{a(1)}$ may have an important effect on lift interference.

V. Wall Interference in a Real Two-Dimensional Wind Tunnel

General Consideration

In this section, the same coordinates system is adopted as in the three-dimensional wind tunnel discussed in the previous sections. An airfoil model is two-dimensional and is spanned between the two side walls. A small perturbation velocity potential $\tilde{\phi}$ in free air can be defined as the potential produced by an airfoil model of infinite span:

$$\tilde{\phi}(x,y,z) = -\frac{1}{2\pi}\int_{x_L}^{x_T} S_2(\xi)\cdot\frac{\xi-x}{(\xi-x)^2+z^2}d\xi + \frac{1}{2\pi}\int_{x_L}^{\infty}[\tilde{\phi}]_-^+\cdot\frac{z}{(\xi-x)^2+z^2}d\xi, \qquad (86)$$

where airfoil thickness is defined as $S_2(\xi)$. ϕ in a two-dimensional wind tunnel is as follows:

$$\begin{aligned}\phi(x,y,z) = &-\frac{1}{2\pi}\int_{x_L}^{x_T} S_2(\xi)\cdot\frac{\xi-x}{(\xi-x)^2+z^2}d\xi \\ &-\frac{1}{2\pi}\int_{x_L}^{x_T} S_2(\xi)\cdot\sum_{n=1}^{\infty}\left\{\frac{\xi-x}{(2Hn+z)^2+(\xi-x)^2} + \frac{\xi-x}{(2Hn-z)^2+(\xi-x)^2}\right\}d\xi \\ &-\int_{x_L}^{\infty}d\xi\int_{-L}^{L}d\eta[\phi]_-^+\cdot\frac{\partial\psi}{\partial\zeta}\Big|_{\zeta=0} \\ &-\iint_Y\{ug+v\psi\}_{-L}^{L}d\xi d\zeta \\ &-\iint_Z[uh+w\psi]_{-H}^{H}d\xi d\eta. \qquad (87)\end{aligned}$$

Even in a two-dimensional test, pressure on an airfoil model usually change spanwise. Moreover, the spanwise pressure change is the greater when uniform stream Mach number is the higher. In this case, the three-dimensional wall correction must be made to measured quantities. But adequate suction from the side walls around a model can make the spanwise pressure change very small in some spanwise region, $y \in [-L', L']$. (See Fig.11.) Then, the side control planes, Σ_L and Σ_{-L}, are taken at $y = L'$ and $-L'$ respectively, and L' is considered as L now. There may be velocity component, v_L^a, on the control surfaces even if the spanwise pressure change in this reion is negligibly small and is also within an accuracy of the small disturbance theory. If this test section has large λ, the lower harmonics of $v_{Lc}^{a(n)}$ and $v_{Ls}^{a(n)}$ may have a great effect on the wall interference. This will be demonstrated in the following. For example, $\varphi_x(x,0,\pm0)$ and $\varphi_z(x,0,\pm0)$ are approximated as follows:

$$\begin{aligned}&\varphi_x(x,0,\pm0) \\ &\simeq \frac{1}{2\pi}\int_{x_L}^{x_T} S_2(\xi)\left\{\frac{\pi^2}{4H^2}\operatorname{cosech}^2\frac{\pi}{2H}(\xi-x) - \frac{1}{(\xi-x)^2}\right\}d\xi \\ &+\frac{1}{4H}\int_{-\infty}^{\infty} w_{Hc}^{a(0)}(\xi)\cdot\tanh\frac{\pi}{2H}(x-\xi)d\xi \\ &+\frac{1}{4L}\int_{-\infty}^{\infty} v_{Lc}^{a(0)}(\xi)\cdot\tanh\frac{\pi}{2L}(x-\xi)d\xi \\ &+\frac{2}{L}\int_{-\infty}^{\infty} v_{Lc}^{a(1)}(\xi)\cdot\sum_{\nu=1}^{\infty}\frac{\frac{x-\xi}{L}}{\sqrt{(2\nu-1)^2+\left(\frac{\xi-x}{L}\right)^2}} \\ &\times K_1\left(\frac{\pi}{\lambda}\sqrt{(2\nu-1)^2+\left(\frac{\xi-x}{L}\right)^2}\right)d\xi, \qquad (88)\end{aligned}$$

$$\begin{aligned}&\varphi_z(x,0,\pm0) \\ &\simeq \frac{1}{4H}\int_{x_L}^{x_T}[u]_-^+d\xi + \frac{1}{24H^2}\int_{x_L}^{x_T}[u]_-^+\cdot(x-\xi)d\xi \\ &-\frac{1}{2H}\int_{-\infty}^{\infty} u_{Hc}^{a(0)}\cdot\frac{1}{1+\exp\{\pi(\xi-x)/H\}}d\xi \\ &-\frac{2}{H}\int_{-\infty}^{\infty} v_{Ls}^{a(1)}\sum_{\nu=1}^{\infty}K_0\left(\frac{\pi}{\lambda}\sqrt{(2\nu-1)^2+\left(\frac{\xi-x}{L}\right)^2}\right)d\xi. \qquad (89)\end{aligned}$$

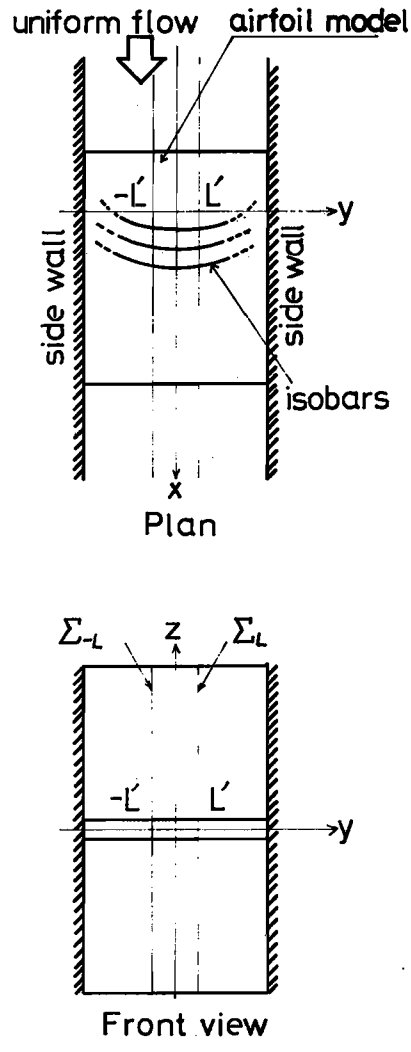

Fig.11 Two-Dimensional Wind Tunnel

Therefore, $v_{Lc}^{a(1)}$ and $v_{Ls}^{a(1)}$ can have a great effect on $\varphi_x(x,0,\pm 0)$ and $\varphi_z(x,0,\pm 0)$ even if they are very small. Consequently, it becomes impossible to evaluate corrections based on such small quantities that are difficult to measure to some degree of accuracy. So L must be as large as possible, and at the same time, v_L^a must be as small as possible.

VI. Experiment in the NAL 2m × 2m Transonic Wind Tunnel

Static pressure distributions along two control lines, which run parallel to the top and bottom walls at the same distance from a model, were measured in the NAL 2m × 2m transonic wind tunnel test section using two rails designed after Ref.(2). They were *4250 mm* long and affixed to the wind tunnel top and bottom walls midway between the tunnel side walls. The test section has perforated walls with normal holes on all four sides, and the open area ratio of them can be arbitrarily varied in the range from *0* to *20* %. In this experiment, the open area ratio of the top and bottom walls was set at *20* %, while that of the side walls was set at *0* % in order to make the test section two-dimensional. Two airfoil models were used in order to fined out whether or not the blockage and the lift interferences depend on airfoil sections. One is Model 70811 which is a shock-free airfoil designed by S. Takanashi.[16] This model is *400 mm* in chord length, *2000 mm* in span, and *10.4* % in thickness ratio. The other is named " Airfoil X " which is not an advanced airfoil but of a conventional design. This model is *350 mm* in chord length, *2000 mm* in span, and *14* % in thickness ratio. This experiment is detailed in Ref.(17).

Assuming the flow in this test section to be two-dimensional, we can substitute zero for v_L^a, $u_{Hc}^{a(m)}$, and $w_{Hc}^{a(m)}$ $(m=1,2,3,\ldots)$ in Eq.(88) and (89). Then

$$\varphi_x(x,0,\pm 0) = -\frac{\pi}{24H^2}\int_{x_L}^{x_T} S_2(\xi)\,d\xi + \frac{\pi^3}{480H^4}\int_{x_L}^{x_T} S_2(\xi)\cdot(\xi-x)^2\,d\xi + \frac{1}{4H}\int_{-\infty}^{\infty} w_{Hc}^{a(0)}(\xi)\cdot\tanh\frac{\pi}{2H}(x-\xi)\,d\xi, \qquad (90)$$

$$\varphi_z(x,0,\pm 0) = \frac{1}{4H}\int_{x_L}^{x_T}[u]_-^+\,d\xi + \frac{\pi}{24H^2}\int_{x_L}^{x_T}[u]_-^+\cdot(x-\xi)\,d\xi - \frac{1}{2H}\int_{-\infty}^{\infty} u_{Hc}^{a(0)}(\xi)\cdot\frac{1}{1+\exp\{\pi(\xi-x)/H\}}\,d\xi. \qquad (91)$$

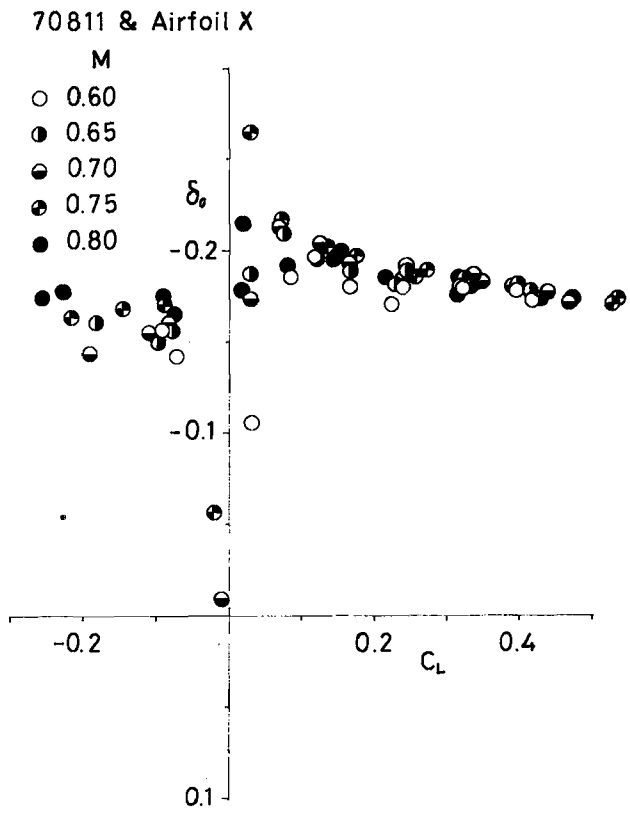

Fig.12-1 δ_0 vs. C_L

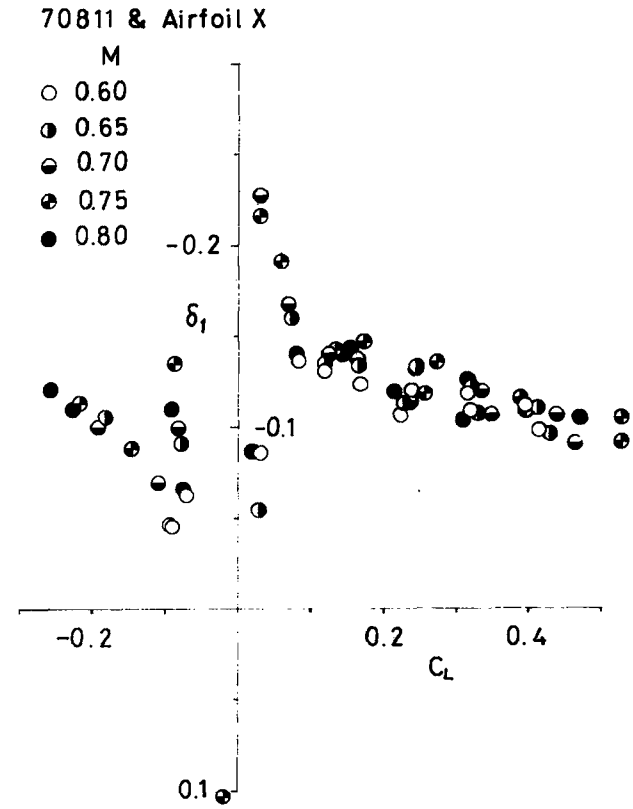

Fig.12-2 δ_1 vs. C_L

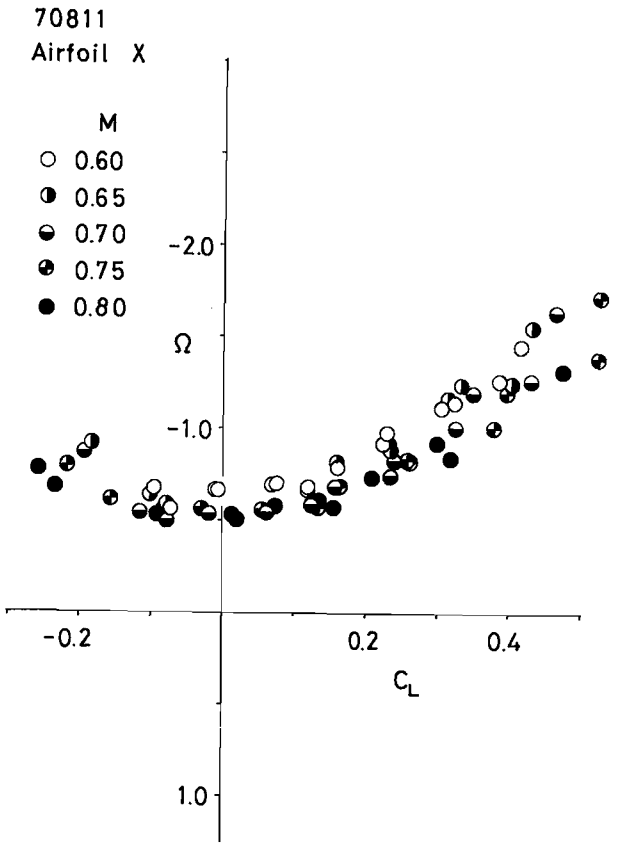

Fig.13 Ω vs. C_L

These equations are equivalent to Eqs.(32) and (34) in Ref.(6). In the same way as in the previous section with subheading Rectangular Test Section with Solid Side Walls, $w_{Hc}^{a(0)}$ can be expressed by $u_{Hc}^{s(0)}$. Therefore, using the static pressure distributions along the control lines, both blockage and lift interference corrections can be estimated. The blockage factor ratio Ω and the lift interference parameters δ_0 and δ_1 are shown in Figs.12 and 13. As can be seen in these figures, the results indicate that these parameters do not depend on the tested airfoils nor Mach number between 0.6 and 0.8, but depend on lift coefficient. Then by the use of the above characteristics, it is possible to make corrections for both the blockage and lift interferences without measuring the pressure distributions every time. Refs.(17) and (18) detail the resulting features of the lift interference parameters and the blockage factor ratio, respectively.

VII. Conclusions

(1) Formulae for the tunnel wall corrections of three-dimensional test section have been established which need the velocity component distributions on four control surfaces, Σ_H, Σ_{-H}, Σ_L, and Σ_{-L} in addition to the pressure distribution on a model.

(2) It is possible to correct test results for wind tunnel wall interference with a sufficient accuracy by the use of the lower harmonic components of $v_{Lc}^{a(n)}$, $v_{Ls}^{a(n)}$, $w_{Hc}^{a(m)}$ and $u_{Hc}^{a(m)}$.

(3) Suction from side walls can have a great effect on wall interference in a two-dimensional wind tunnel. The distance over which the pressure on an airfoil model does not change spanwise must be made as long as possible by means of suction from side walls, but the suction velocity must be as small as possible at the same time.

(4) The blockage factor ratio Ω and the lift interference parameters δ_0 and δ_1 depend on lift coefficient of a model but not so sensitively on the difference in the tested airfoil sections nor uniform Mach number between 0.6 and 0.8. Consequently, it is possible by the use of the above characteristics to make corrections without measuring the pressure distributions near the walls each time.

Acknowledgement

The present author gratefully acknowledges the continued encouragement of Dr. H. Endo, director of the 2nd aerodynamics division, National Aerospace Laboratory, Japan.

References

(1) Ebihara, M. : A Study of Subsonic Two-Dimensional Wall-Interference Effects in a Perforated Wind Tunnel with Particular Reference to the NAL 2m ×2m Transonic Wind Tunnel Inapplicability of the Conventional Boundary Condition, NAL TR-252T, January, 1972

(2) Mokry, M., Peak, D. J., and Bowker, A. J. : Wall Interference on Two-dimensional Supercritical Airfoils, Using Wall Pressure Measurements to Determine the Porosity Factors for Tunnel Floor and Ceiling, NRC LR-575, 1974

(3) Kacprzynski, J. : Transonic Flow Field past 2-D Airfoils between Porous Wind Tunnel Walls with Nonlinear Characteristics, AIAA Paper No. 75-81, 1975

(4) Kemp, W. B. : Toward the Correctable Interference Transonic Wind Tunnel, Proceedings of the AIAA 9th Aerodynamic Testing Con erence, June, 1976, pp.31-38

(5) Capelier, C., Chevellier, J. -P., and Bouniol, F. : Nouvelle Methode de Correction des Effects de Parois en Courant Plan, La Recherche Aerospatiale, Jan.-Feb., 1978, pp.1-11

(6) Lo, C. F. : Tunnel Interference Assessment by Boundary Measurements, AIAA Journal, Vol.16, 1978, pp.411-413

(7) Sawada, H. : A General Correction Method of the Interference in 2-Dimensional Wind Tunnels with Ventilated Walls, Transactions of the Japan Society for Aeronautical and Space Sciences, Vol.21, 1978, pp.57-68

(8) Sawada, H. : A General Correction Method of the Interference in 3-Dimensional Wind Tunnels with Ventilated Walls, NAL TR-545, September, 1978

(9) Mokry, M., and Ohman, L. H. : Application of the Fast Fourier Transform to Two-Dimensional Wind Tunnel Wall Interference, Journal of Aircraft, to be published.

(10) Blackwell, J. A. : Wind Tunnel Blockage Correction for Two-Dimensional Transonic Flow, Journal of Aircraft, Vol.16, 1979, pp.256-263

(11) Murman, E. M. : A Correction Method for Transonic Wind Tunnel Wall Interference, AIAA Paper 79-1533, July, 1979

(12) Kemp, W. B. : Transonic Assessment of Two-Dimensional Wind Tunnel Wall Interference Using Measured Wall Pressure, Advanced Technology Airfoil Research, pp.473-486, NASA Conference Publication 2045, March, 1978

(13) Garner, H. C. : Lift Interference on Three-Dimensional Wings, AGARDograph 109, October, 1966, pp.75-218

(14) Rogers, E. W. E. : Blockage Effects in Closed or Open Tunnels, AGARDograph 109, October, 1966, pp.279-340

(15) Vayssair, J. : Survey of Methods for Correcting Wall Constraints Transonic Wind Tunnels, AGARD-R-601, 1973

(16) Takanashi, S. : A Convergence Theorem of Nonlinear Semigroups and its Application to First Order Quasilinear Equations, NAL TR-318T, 1973

(17) Sawada, H. : An Experiment of Lift Interference on 2-Dimensional Wings in a Wind Tunnel with Perforated Walls, Transactions of the Japan Society for Aeronautical and Space Sciences, Vol.22, No.58, 1980

(18) Sawada, H. : A New Method of Calculating Corrections for Blockage Effects in Two-Dimensional Wind Tunnel with Ventilated Walls, Using Wall Pressure Measurements, Transactions of the Japan Society for Aeronautical and Space Sciences, to be published.